

Shockwave and cavitation bubble dynamics of atmospheric air

Ch. Leela¹, S. Bagchi², Surya P. Tewari¹ and P. Prem Kiran¹

¹ *Advanced Center of Research in High Energy Materials (ACRHEM), University of Hyderabad, Hyderabad, A.P. 500046, India*

² *Currently at Raja Ramanna Centre for Advanced Technology, Indore, M.P. 452013, India*

Abstract. The generation and evolution of laser induced shock waves (SWs) and the hot core plasma (HCP) created by focusing 7 ns, 532 nm laser pulses in ambient air is studied using time resolved shadowgraphic imaging technique. The dynamics of rapidly expanding plasma releasing SWs into the ambient atmosphere were studied for time delays ranging from nanoseconds to milliseconds with ns temporal resolution. The SW is observed to get detached from expanding HCP at around 3 μ s. Though the SWs were found to expand spherically following the Sedov-Taylor theory, the rapidly expanding HCP shows asymmetric expansion during both the expansion and cooling phase similar to that of inertial cavitation bubble (CB) dynamics. The asymmetric expansion of HCP leads to oscillation of the plasma boundary, eventually leading to collapse by forming vortices formed by the interaction of ambient air.

1. INTRODUCTION

An efficient coupling of laser energy to the target is an essential aspect of Inertial Confinement Fusion (ICF) scheme in which there is a need to characterize small nonuniformities in shock compressed materials. Laser-driven Shock Waves (SW's) characterized by several optical methods provide Equations of State (EOS) for a variety of materials used in high-energy density physics experiments at Mbar pressures [1–3]. In addition to the EoS studies, laser induced shockwaves (LISW) have many applications such as laser surface cleaning [4] of the viewports for high repetition rate reactors employed in main vacuum vessel of ICF and in improving the fatigue life of materials via laser shock peening [5]. In all these studies coupling of laser energy into the material and the evolution of laser induced plasma plays a crucial role. The crucial issue involved in efficient coupling of optical energy is the interaction of high power laser beams with materials, which is an intriguing field of research owing to the nonlinear optical properties coming to the fore during laser-matter interaction. In the study of laser induced shockwaves in ambient conditions and in under dense plasmas, the existing theoretical and experimental reports mostly consider the SWs emanate from a single point source [6–8] and neglects the self-focusing of laser pulses interacting with the plasma. To address this issue, we present our results from the SHW imaging technique revealing the dynamics of LISW and hot core plasma (HCP) from LPP in air generated with 7 ns laser pulses which gives the full spatial information of the evolution of the position of SW fronts and expansion of the hot gas. Our experimental results reveal the existence of multiple sources with minimum gate width of 1.5 ns which clearly shows the asymmetric expansion of the SW and HCP.

2. EXPERIMENTAL DETAILS

The dynamics of LISW and HCP were studied using time resolved SHW imaging technique as shown in Figure 1. Laser pulses from second harmonic of Nd: YAG laser (Innolas Spotlight-1200) focused in

This is an Open Access article distributed under the terms of the Creative Commons Attribution License 2.0, which permits unrestricted use, distribution, and reproduction in any medium, provided the original work is properly cited.

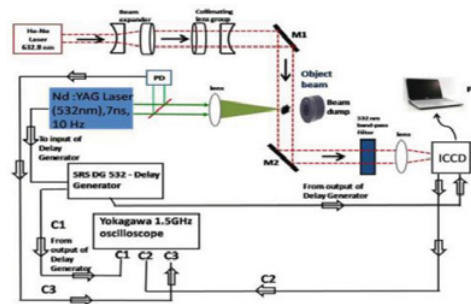


Figure 1. Experimental schematic of shadowgraphy and synchronization of ICCD camera with the laser pulse.

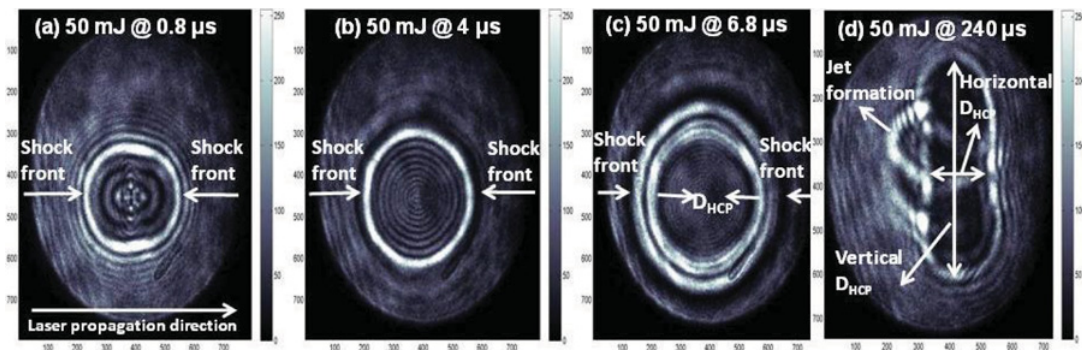


Figure 2. Shadowgram showing SW and CB at (a) $0.8 \mu\text{s}$ (b) $4 \mu\text{s}$ (c) $6.8 \mu\text{s}$ and (d) $240 \mu\text{s}$ for 50 mJ.

$f/10$ geometry at 50 mJ input laser energy is used to generate LPP in air launching SWs into ambient atmosphere. He-Ne laser beam (CW, 25 mW, CVI Melles Griot) is used as probe beam. The gate width of the ICCD camera (ANDOR DH-734) which is fixed at 1.5 ns was synchronized and delayed with respect to the plasma generating laser pulse with the help of delay generator in order to capture the LISW and HCP. The time delay between the laser pulse, ICCD gate width is monitored using a digital oscilloscope. A band pass filter centered at 632 nm is placed in front of the ICCD to eliminate the background illumination. The shadowgrams were captured at regular time delays from 0.2 to 1100 μs .

3. RESULTS AND DISCUSSIONS

Figure 2(a)–(d) shows the shadowgrams at 0.8, 4, 6.8 and 240 μs delays from “ $t = 0$ ” respectively. The position of Shock Front (SF) at different delays from the time laser interacts with the material is a measure of the shock velocity. The laser propagation direction is from left to right. From the images, SF, a dark layer can be clearly seen along with the boundary of the HCP, a white layer. D_{HCP} indicates the diameter of the HCP.

Most of the absorbed laser energy is irreversibly converted to heat and remains deposited in the focal volume. Center dark region in the shadowgrams is due to high density and temperature gradients. In addition to the SF and HCP, many internal fringes representing the superposition of partially refracted probe beam and the unperturbed part of the probe beam were observed till the delay of 6.4 μs . The SF gets detached from the HCP at around 3.2 μs after which the SW propagates in to ambient atmosphere. The radial position of SF, R_{SW} is measured from the series of shadowgrams at different delays (Figure 3(a)).

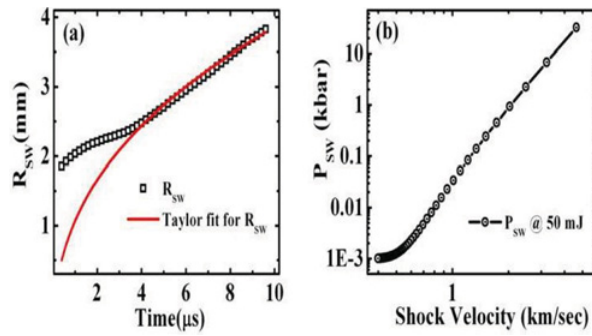


Figure 3. (a) SW location data showing radius of curvature of shock front (R_{SW}) and solid line showing the curve fit to Taylor solution. (b) P-U Hugoniot of air at 50 mJ laser energy.

Following the Sedov-Taylor solution and Counter Pressure Corrected Point Strong Explosion Theory (CPC-PSET), the radius of curvature of SF (R_{SW}) [9, 10] can be expressed as $R_{SW} = \Phi_0 (E_{SW} t^2 / \rho_0)^{1/5}$ where E_{SW} is the energy released by the plasma that drives the SW, t is the time elapsed since the origin of the plasma, ρ_0 is the density of the ambient medium and Φ_0 is a constant dependent upon the specific heat ratio, γ , of the ambient medium, taken as 1 in case of air. Figure 3(a) shows the evolution of R_{SW} as a function of delay from the laser pulse with E_{SW} as a fitting parameter. The velocity of SF is slower in the initial time scales and getting saturated by $3.2 \mu s$ after which the velocity is observed to be higher. The evolution of the SW follows Sedov-Taylor solution at longer time scales $> 3.2 \mu s$ following the spherical nature whereas it deviates at smaller time delays $< 3.2 \mu s$. Around the same time the SW is observed to detach from the HCP and propagate into ambient atmosphere (Figures 2(b) and (c)). The expanding SW is observed for time delays up to $10 \mu s$ above which the SW leaves the field of view. Maximum and minimum R_{SW} was observed to be 1.8 and 3.8 mm respectively over a delay of $9.6 \mu s$. Assuming the ambient pressure is negligible with respect to the pressure behind the SW, the gas motion is determined by two parameters, E_W and ρ_0 . The instantaneous propagation speed of the spherical shock (V_{SW}) is calculated by differentiating equation R_{SW} with respect to time. The V_{SW} rapidly decays from a maximum value of 4.6 km/sec to approximately 0.4 km/sec. From V_{SW} , pressure of the air behind the SF (P_{SW}) [9] were calculated using $P_{sw} = P_0 + \rho_0 v_s^2 (1 - \rho_0/\rho)(M - 1)^2$; where P_0 is the atmospheric pressure (0.1 MPa), v_s is the velocity of sound in air (346 m/sec), $M_{SW}(V_{SW}/v_s)$ is Mach of SW, ρ/ρ_0 is density jump. The V_{SW} and the estimated P_{sw} are used to generate P-U Hugoniot of air (Figure 3(b)).

Though the PSET is able to explain the spherical propagation of SW at larger distances from the origin, it fails to explain the nature of SW's close to the source of explosion (around the focal volume of the lens) (Figure 3(a)). This may be due to the presence of two distinct sources of SWs observed in the shadowgrams at the initial time delays (Figure 2(a)) due to a well-known self-focusing of high power beams leading to multiple laser induced breakdown points that initiate plasma generation [11]. The presence of two or multiple sources ensures that the propagation of LISW need to be considered as two or multi centered phenomenon rather than a single center problem.

Analogy between hot core plasma (HCP) and cavitation bubble (CB) dynamics

Though the LISW is expanding symmetrically after $3.2 \mu s$ delay from the laser pulse, following a well-known Sedov-Taylor solution and CPC-PSET, the boundary of the HCP is observed to evolve in an asymmetric fashion with time. At smaller time delays from $t = 0$, the HCP appeared as an oblate along the propagation direction of plasma generating laser pulse till $3.2 \mu s$. The HCP is observed to become almost spherical during $3.2 \mu s$ to $15 \mu s$. Beyond $20 \mu s$, the HCP starts to assume a prolate shape

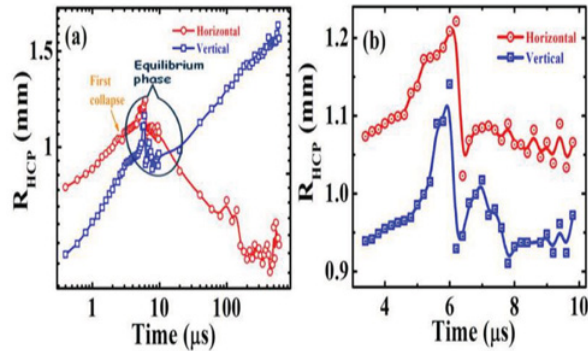


Figure 4. (a) Evolution of radius of the HCP (R_{HCP}) over the entire time delays observed and (b) Expanded view of the evolution R_{HCP} during equilibrium phase (oscillation phase) immediately after detachment of SF from HCP oscillating analogous to that of an elliptic CB. Lines are guide to the eye.

(Fig 2(d)). The radius of the HCP (R_{HCP}) is observed to vary from 0.56–1.22 mm along the horizontal direction and from 0.63–1.7 mm in the vertical direction clearly indicating the eccentricity (fig. 4(a)). After the first collapse of HCP, the boundary of HCP rebounds and the process repeats itself in the form of oscillations and then the HCP breakdown takes place. At $3.2 \mu\text{s}$, when the SW detaches from the HCP due to gas heating with a more symmetrical spherical shape and continues to expand till $6 \mu\text{s}$ and then cool leading to the first collapse of the bubble at $6.2 \mu\text{s}$ (Figure 4(b)).

The observed dynamics of HCP are closer to that of an elliptical cavitation bubble (CB) [12] observed during laser interaction with fluids [13]. At later time scales of $160 \mu\text{s}$, we observe the jet formation (Figure 2(d)) and subsequent penetration of colder ambient air into the HCP, leading to the rapid oscillations till $1100 \mu\text{s}$ due to the modified pressure gradient, eventually leading to collapse of HCP. The energy of hemispherical HCP [14] is observed to be 3 mJ.

4. CONCLUSIONS AND FUTURE DIRECTION

SHW imaging is used to study the LISW and HCP dynamics in air with ns temporal resolution giving a valuable insight into the laser induced gas dynamic flow. Although the SW's were found to be expanding spherically following Sedov-Taylor model of a point like explosion, the rapidly expanding HCP has shown a clear asymmetry similar to that of an elliptic CB, both while expanding and cooling down to the ambient condition. The maximum V_{SW} and maximum P_{SW} are measured to be 4.6 km/sec and 32 kbar respectively. Further investigations are being carried out to understand the evolution of plasma in the initial time scales in the presence of multiple breakdown sources and their interaction leading to asymmetric behavior of HCP analogous to well-known CB in fluids.

Authors acknowledge DRDO for funding.

References

- [1] R.P. Drake, *High-Energy Density Physics* (Springer-verlag, 2006)
- [2] R.F. Trunin, *Shock Compression of Condensed Materials* (Cambridge University Press, London, 1998)

- [3] D. Batani, A. Balducci, D. Beretta, A. Bernardinello, T. Lower, M. Koeing, A. Benuzzi, B. Faral, and T. Hall, *Phys. Rev. B* **61**, 9287 (2000)
- [4] B. Luk'yanchuk., *Laser surface cleaning* (World Scientific Publishing Co. Pte, Ltd, 2002)
- [5] K. Ding and L. Ye., *Laser shock peening performance and process simulation* (Woodhead Publishing Limited, 2006)
- [6] B. Wang, K. Komurasaki, T. Yamaguchi, K. Shimamura, and Y. Arakawa, *J. Appl. Phys.* **108**, 124911 (2010)
- [7] M. Thiyagarajan, and J. Scharer, *J. Appl. Phys.* **104**, 013303 (2008)
- [8] I.G. Dors, C.G. Parigger, *Appl. Optics* **42**, 5978 (2003)
- [9] S.H. Jeong, R. Greif and R.E. Russo, *Appl. Surf. Sci.* **127**, 1029 (1998)
- [10] Ya. B. Zel'dovich and Yu.P. Raizer, *Physics of SWs and High-Temperature Hydrodynamic phenomena* (Dover Publications, 2002)
- [11] V.V. Krokobin and A.J. Alcock, *Phys. Rev. Lett.* **21**, 1433 (1968)
- [12] K. Y. Lim, P.A. Quinto-Su, E. Klaseboer, B.C. Khoo, V. Venugopalan and C-D. Ohl, *Phys. Rev. E* **81**, 016308 (2010)
- [13] W. Lauterborn and T. Kurz, *Rep. Prog. Phys.* **73**, 106501 (2010)
- [14] K. R. Rau, P. A. Quinto-Su, A. N. Hellman, V. Venugopalan, *Biophys. J.* **91**, 317 (2006)